

Diffusion-Reinforcement Learning Hierarchical Motion Planning in Multi-agent Adversarial Games

Zixuan Wu*, Sean Ye*, Manisha Natarajan* and Matthew C. Gombolay*

Abstract—Reinforcement Learning (RL)-based motion planning has recently shown the potential to outperform traditional approaches from autonomous navigation to robot manipulation. In this work, we focus on a motion planning task for an evasive target in a partially observable multi-agent adversarial pursuit-evasion game (PEG). Pursuit-evasion problems are relevant to various applications, such as search and rescue operations and surveillance robots, where robots must effectively plan their actions to gather intelligence or accomplish mission tasks while avoiding detection or capture. We propose a hierarchical architecture that integrates a high-level diffusion model to plan global paths responsive to environment data, while a low-level RL policy reasons about evasive versus global path-following behavior. The benchmark results across different domains and different observability show that our approach outperforms baselines by 77.18% and 47.38% on detection and goal reaching rate, which leads to 51.4% increasing of the performance score on average. Additionally, our method improves interpretability, flexibility and efficiency of the learned policy.¹

I. INTRODUCTION

Multi-agent pursuit-evasion games (PEG) [1] are ubiquitous in real-world robotics scenarios, where robotic systems could be applied to drug smuggler tracking [2], defensive escorting [3], or robot soccer [4]. In PEG, one team seeks to track its target while the target agent or team employs evasive maneuvers, and research naturally focuses on developing methods for either the pursuers [5] or evaders [6]–[8]. Although there has been extensive work on developing search policies [9]–[11], relatively little attention has been paid to evasion. This lack of emphasis provides an opportunity to design a novel evasive policy that is useful in real-world scenarios, such as business ships evading pirates and evacuating lost people in national parks.

Recently, learning-based methods, such as Graph Neural Networks [12], diffusion models [13] or reinforcement learning (RL) methods [14] have been widely used in the pursuit-evasion games and similar navigation problems [15]–[17] (e.g. goal-reaching, path-planning, etc.). These methods often outperform expert policies [18]. However, learning the RL policy is usually subject to two key challenges—partial observability and high sample complexity when exploring large-scale, partially observable environments, as considered in our work.

Researchers propose hierarchical approaches to help exploration by structuring the goal, policies, or rewards. Goal-

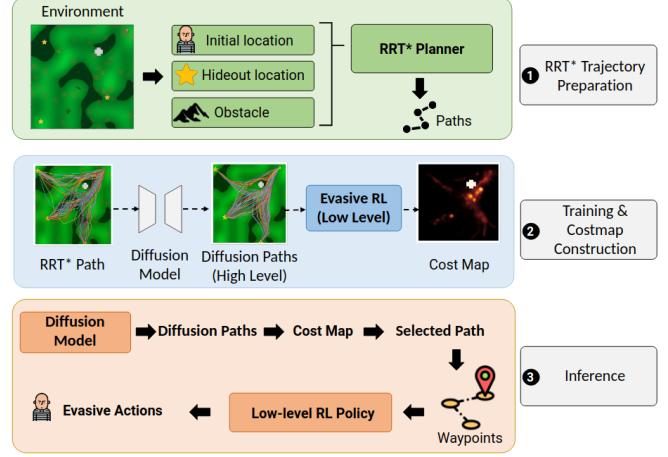


Fig. 1. Diffusion-RL Framework Overview: We first collect RRT* paths into a dataset. Then we use a diffusion model to learn the distribution of the RRT* path and generate samples as the high-level global plans to help learn a low-level evasive RL policy. A posterior costmap is built based on the learned hierarchy and detection risk and can be used to select the best global path in the inference stage.

oriented reinforcement learning (for example, a replay of the hindsight experience [19]) increases the reward density by assuming that the goal has been reached in each exploration trajectory and corrects observation and reward accordingly. Hierarchical RL [20] improves sample efficiency from spatial or temporal abstraction by multiple hierarchically organized RL policies, and hybrid reward structure-based methods [21] try to capture the multimodal distribution of reward where each part of the value function can be a low-dimensional representation. However, their applications are tested in fully observable games [20] or require expert prior knowledge as primitives [22].

In this paper, we propose a novel hierarchical learning framework that combines diffusion and RL as high- and low-level policies, respectively. The diffusion model is used as a global path generator to satisfy static map constraints, such as terminal states and obstacle avoidance. Furthermore, we employ a low-level RL policy that learns to follow the waypoints while prudently evading captures (see Figure 1). Our key insight is that using the diffusion model can improve the RL performance by constraining its exploration to high-value state-action regions and can help downstream tasks by providing diverse options. *We find our method is especially useful for the evader to learn escaping behaviors in the large multi-agent, multi-goal partially observable settings — Prisoner Escape and Narco Interdiction Domain (see §III-B).*

Contributions: In summary, our contributions are three-fold:

* Authors are from the Institute of Robotics and Intelligent Machines (IRIM), Georgia Institute of Technology, Atlanta, GA 30308, USA.

Correspondance Author: Zixuan Wu zwu380@gatech.edu

¹Code and supplementary details are at https://github.com/ChampagneAndFragrance/Diffusion_RL

- 1) We propose a novel hierarchical system consisting of a diffusion model as a high-level global path planner to aid RL exploration and a low-level RL agent to learn evasive maneuvers, which outperforms all baselines.
- 2) We design an algorithm to implicitly infer the cost map that is used to select paths within our hierarchical motion planning framework to evade the searching agents. Multiple ablation studies show the interpretability, flexibility, efficiency, and generalizability of our method.
- 3) Our work is the first to equip evaders with hierarchical motion planning to learn escaping while reaching the navigation goal in large partially observable environments without expert primitives.

II. RELATED WORK

A. Pursuit-Evasion Games

A perfect information PEG (i.e., full observability) can be modeled as a differential game and solved using control theory [23]. In comparison, the incomplete information PEG (i.e., partial observability) is a more realistic setting since agents usually do not have full knowledge of the environment at all time. Researchers commonly use probabilistic models [24], [25] and formulate PEG as optimization problems to maximize the payoff [26], [27]. Therefore, recent research also focuses on obtaining the optimal policy through RL [28]. Unfortunately, most RL works focus on pursuit policies [29], [30]. Some recent works [31], [32] have focused on evasive behaviors evolved from scratch, but these policies do not need to reach explicit navigation goals. In comparison, we derive an evader policy that can not only escape from pursuers but also reach goals in large, adversarial, and partially observable domains.

B. Diffusion Models in Path Generating

Diffusion models are a class of generative models that have demonstrated impressive performance in generating sequential data in several applications, such as image synthesis and video generation [33]–[35]. Recently, there have been several works employing diffusion models in trajectory generation tasks. Diffuser [36] trains a diffusion model for trajectory generation on offline datasets and plans future trajectories with guided sampling. The diffusion policy extends this work to imitation learning and demonstrates the ability to learn robust policies for various pushing tasks conditioned only on visual input [37]. Recent work [13] has extended these approaches for generating trajectories of multiple opponents. In our work, we further use the diffusion model as a trajectory planner that allows the reinforcement learning agent to generate diverse plan options in our partially observable pursuit-evasion domain.

C. RL in Motion Planning

Recent work has demonstrated the success of RL for motion planning problems in dynamic environments [15], [38]–[40]. Many papers discuss how to use RL to avoid obstacles by analyzing exteroceptive sensor information such as RGB cameras [40], LIDARs [39], [40], or converted laser data

from images [38]. However, none of these previous works assumes an adversarial environment where the “obstacles” are intelligent pursuers, or the map is as large as in our scenario with undetectable parts.

The work [15] also employs a hierarchical structure in goal-conditioned planning; however, their environment does not incorporate adversaries or multiple goals, and their RL policy is not trained from scratch. Dynamic obstacles are considered in [41]; however, these obstacles can only run on a predefined segment with a constant velocity, and the map is known such that A* search can be sufficient to find the optimal path. In our scenario, we assume the cameras are hidden from the evader in a non-discovered terrain map, while the pursuit team can use these cameras to detect and track the evader.

III. ENVIRONMENT

A. Partially Observable Markov Decision Process

We model adversarial search and tracking as a Partially Observable Markov Decision Process (POMDP). A POMDP for an agent can be defined by a state s , private observation o , action a , and a transition function $\mathcal{T} : s \times a \mapsto s$. At each timestep t , an agent receives an observation o^t , chooses an action $a^t \in \mathcal{A}$, and obtains a reward $r^t : s \times a_i \mapsto \mathbb{R}$. The initial world state is drawn from a prior distribution ρ . In our environment (see §III-B), we assume that the evader starts from a random position from a corner region of the map while the pursuit team starts from random positions on the map. It is a partially observable environment for the evader in that 1) cameras are invisible to the evader, 2) the terrain map is not provided a priori, and 3) the evader may only have a limited detection range.

B. Prisoner Escape and Narco Interdiction

In our evaluation of the proposed algorithm, we employ two open-sourced large-scale pursuit-evasion domains [12] named Prisoner Escape and Narco Interdiction (Figure 2). In both domains, an evader (prisoner or smuggler) is being tracked by a team of search agents in a partially observable environment. In each episode, three hideouts are drawn from all candidate hideouts. These hideouts are only visible to the evader and unknown to the pursuit team, as adversarial teams do not communicate intent. The terminal objective of the evader is to reach any hideout on the map (considered a success) or reach the time limit (considered a failure). Simultaneously, the evader should learn to avoid pursuit team detection. The heterogeneous pursuit team consists of static (cameras) and dynamic agents (search parties, helicopters, search boats, and planes) that collaborate to search and track the evader in both domains.

The maximum speed of the evader is always lower than the pursuit agents, making it more challenging for the evader to plan evasive maneuvers to successfully reach the hideouts undetected. The observation of the evader includes the current timestep, hideout locations, mountain locations, pursuer states, and evader states. The evader can see the pursuer anywhere in the global-view mode and within a field-of-view in

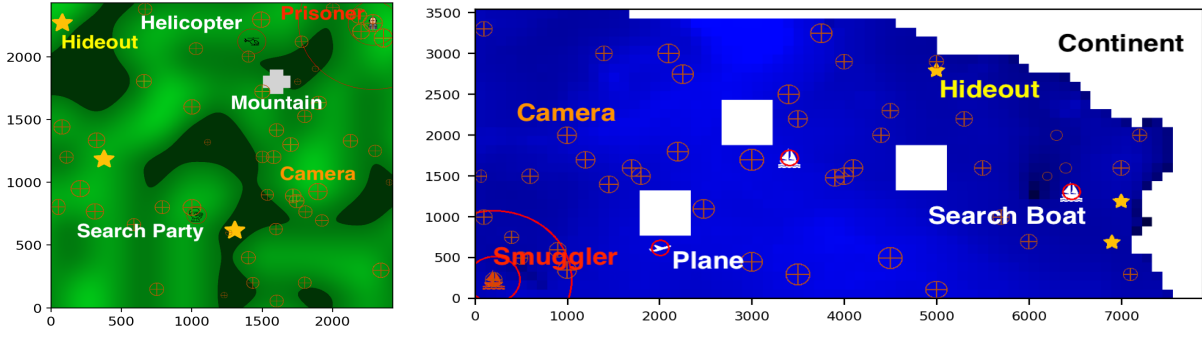


Fig. 2. Prisoner Escape Domain (left) and Narco Traffic Interdiction Domain (right)

the local-view mode, and the camera locations and visibility map are always hidden from the evader. In the local-view mode, evader's field-of-view, d_e , is parameterized by the searching agent type, β_{type} , visibility, c_v , and searching agent speed, s_s : $d_e = \alpha \cdot (\beta_{type} \cdot c_v \cdot s_s + \eta)$. These domains increase the complexity of the task and more closely match real-world dynamics compared to other pursuit-evasion games [23], [42], [43].

C. Pursuit Team Behavior

To provide a fair comparison between our evading algorithm and the baselines, we use a fixed heuristic policy for the pursuit team inspired by prior works [44], [45] that achieved good performance in the prisoner escape domain [14]. The search agents can choose to either 1) go to the last detection, 2) search along the predicted path, or 3) search in the vicinity of the last detection. Searching team detection range, d_s , is parameterized by the agent type, β_{type} , visibility, c_v , and evader speed s_e : $d_s = \alpha \cdot (\beta_{type} \cdot c_v \cdot s_e + \eta)$, which means a higher visibility and evader speed will lead to larger detection range. The pursuer policy is designed to effectively utilize the available information and adapt to different scenarios.

IV. METHOD

The evader's objective is to reach one of the hideouts on the map and evade detection by the pursuit team, using only partial map knowledge, without any information about camera locations or models for whether the pursuers can detect the evader. RL or diffusion-based motion planning each partially fits our setting: RL can hypothetically learn to evade through trial-and-error. However, RL has difficulties with exploration in the large, adversarial, and multi-goal domains. On the other hand, diffusion-based motion planning can generate diverse plans that reach the goals; however, diffusion models struggle to learn evasive behaviors and avoid the pursuing agents. The reason is that the diffusion model has a relatively long denoising process that is difficult to handle environment dynamics. Additionally, partial observability induces high variance in training.

We propose to leverage the strengths of diffusion and RL policies by using diffusion models to guide RL exploration during training and generate path candidates at inference. We decompose the hierarchy into the following: learning diffusion-based global plans that meet start, terminal, and obstacle constraints from RRT* paths (§IV-A), employing

RL local evasive behaviors to avoid detection en-route (§IV-B), and path selection from posteriorly constructed costmap during inference (§IV-C).

Algorithm 1: Diffusion Model Training

Data: Start Location \mathcal{S} , Goal Locations \mathcal{G} , Obstacle Location \mathcal{M} , Constraints $\mathcal{C} = \langle \mathcal{S}, \mathcal{G}, \mathcal{M} \rangle$, Data buffer \mathcal{D} , Noise Scheduling Terms $\alpha_i, \bar{\alpha}_i$, Learning Rate α , Denoising Timesteps T

Result: Diffusion Model s_θ

```

1 while buffer  $\mathcal{D}$  not full do
2    $c = \langle p_s, p_g, m \rangle \sim \mathcal{C}$  ;  $\triangleleft$  Draw global constraints
3    $\tau \leftarrow \text{RRT}^*(c)$  ;  $\triangleleft$  Plan RRT* path
4    $\tau \leftarrow \text{Sample}_{\downarrow}(\tau)$  ;  $\triangleleft$  Uniformly downsample path
5    $\mathcal{D} \leftarrow \tau, c$  ;  $\triangleleft$  Store trajectory, constrains in dataset
6 while not converged do
7    $\triangleleft$  Draw  $\tau, c$  diffusion timestep, and random noise
8    $\tau_0, c \sim \mathcal{D}$  ;  $i \sim \mathcal{U}(1, T)$ ,  $\epsilon \sim \mathcal{N}(0, I)$ ;
9    $\triangleleft$  Compute Score Matching MSE Loss
10   $\tau_i \leftarrow \sqrt{\bar{\alpha}_i} \tau_0 + \sqrt{1 - \bar{\alpha}_i} \epsilon$ ;
11   $\mathcal{L}(\theta) = \|\epsilon - s_\theta(\tau_i, i, c)\|_2^2$ ;
12   $\triangleleft$  Update Model
13   $\theta = \theta + \alpha \nabla_{\theta} \mathcal{L}(\theta)$ 

```

Algorithm 2: Diffusion Path Generator π^d

Data: Constraints \mathcal{C}

Result: Global plan τ^0

```

1 while  $\tau^0$  not satisfies constraints  $\mathcal{C}$  do
2    $\tau^T \leftarrow$  sample from  $\mathcal{N}(0, I)$  ;  $\triangleleft$  Gaussian Noise
3   for all  $i$  from  $T$  to 1 do
4      $(\mu^i, \Sigma^i) \leftarrow s_\theta(\tau^i), \Sigma_\theta(\tau^i)$ 
5      $\tau^{i-1} \sim \mathcal{N}(\mu^i, \Sigma^i)$  ;  $\triangleleft$  Diffusion Denoise
6      $\tau^{i-1} \leftarrow \mathcal{C}(\tau^{i-1})$  ;  $\triangleleft$  Apply Constraints
7 Return  $\tau^0$ 

```

A. Diffusion Based Global Plan

In this section, we describe how we leverage diffusion models as a generative motion planner to provide a prior for the RL agent to traverse in large, partially observable, and adversarial environments [46]. We utilize a diffusion model

to clone the distribution from RRT* planner and generate waypoints of diverse candidate paths that the agent should follow approximately. This diffusion path planner guides the exploration, increases the sample-time efficiency, and improves the flexibility of the downstream RL algorithm. *The underlying insight is to constrain the RL exploration at a promising distribution implicitly encoded by the diffusion model considering the map constraints.*

The diffusion path planning should have three key attributes: 1) global constraints are satisfied (start and terminal locations, obstacles, etc.); 2) generated plans are diverse and multimodal and 3) the sampling time of the diffusion model is low. We guide the diffusion sampling procedure using constraint guidance [13] to best satisfy the constraints and use a small number of sampling timesteps to keep the sampling time low. The low sampling time allows us to run the diffusion model during the RL training procedure, which is difficult for traditional search-based planners. Additionally, the parallel sampling reduces the overhead at inference time and provides diverse candidates for the agent to use.

We outline the diffusion training process in Algorithm 1. We first generate paths with RRT* (Line 3) — a sample-based motion planner that yields varied paths even for the same initial and target states, which enables the diffusion model to similarly generate diverse paths. Then we uniformly downsample the path into sparse waypoints (Line 4) and train a diffusion model based on these waypoints (Line 6-10). Generating a path with a few waypoints is sufficient enough to act as the high-level planner as we expect the RL policy to act as the low-level dynamic actor to move between waypoints. Generating fewer waypoints also allows sampling time to be faster, which is crucial for training in an RL loop.

The sampling process is summarized in Algorithm 2 with diffusion path generator, π^d . We apply global constraints at each denoising step (Line 6) to help generate a valid path from start to goal.

Algorithm 3: Adversarial Behavior Learning

Data: Initial state s_0 , Diffusion Global Planner π^d , SAC replay buffer \mathcal{D}_s
Result: SAC low-level policy π^{l*}

```

1 while training episodes do
2    $\{w_i\}_{i=0}^{N_w} = \mathbf{w} \sim \pi^d(\mathbf{w}|s_0)$ ;  $\triangleleft$  Waypoints from  $\pi^d$ 
3   while  $w_i$  not reached do
4      $O_{aug} \leftarrow [O|w_i]$ ;  $\triangleleft$  Concat current waypoint
5      $a \sim \pi^l(a|O_{aug})$ ;  $\triangleleft$  Action from low policy
6      $O'_{aug}, r \leftarrow \text{EnvStep}(a)$ ;  $\triangleleft$  Update env
7      $\mathcal{D}_s \leftarrow \{O_{aug}, a, O'_{aug}, r\}$ ;  $\triangleleft$  Push to buffer
8     if  $w_i$  reached then
9        $i \leftarrow i + 1$ ;  $\triangleleft$  Update to next waypoint
10   $\pi^{l*} \leftarrow \text{SAC}(\mathcal{D}_s \sim \mathcal{D}_s)$ ;  $\triangleleft$  Update SAC parameters

```

B. RL Based Adversarial Behavior Learning

In addition to our diffusion model considering the global objectives, it is also essential to design an algorithm directly interacting with the environment that can not only accomplish the tasks from the high-level planners but also capture the dynamic patterns in the map to achieve the local adversarial detection avoiding goals. Although evading heuristics exist [12], we believe that a data-driven reinforcement learning algorithm is a more convenient way compared with the hand-crafted policy and can perform better within specific environment distribution.

Therefore, we employ an RL algorithm Soft Actor-Critic (SAC) as the low-level policy with the following aims: 1) approximately follow the waypoints from the diffusion path and 2) adapt the evader velocities to escape from searching agents. We summarize RL training in Algorithm 3 where we augment the observation with the current desired waypoint from the high-level planner (Line 2, 4). The training objective can be formulated as Equation (1) where \approx means a similar low-level policy can be derived from both sides.

$$\begin{aligned}
R &= \max_{\pi} \mathbb{E}_{\pi} \left[\sum_t \gamma^t \cdot r \right] \\
&\approx \max_{\pi^g} \mathbb{E}_{\pi^g} \left[\max_{\pi^l} \mathbb{E}_{\pi^l} \left[\sum_{\tau=0}^{t_g} \sum_{t=0}^{t_l} \gamma^t \cdot r \mid w^{\tau} \sim \pi^g(w|s^{\tau}) \right] \right] \\
&\approx \max_{\pi^l} \mathbb{E}_{\pi^l} \left[\sum_{\tau=0}^{t_g} \sum_{t=0}^{t_l} \gamma^t \cdot r \mid \mathbf{w} \sim \pi^d(\mathbf{w}|s_0), s_0 \sim \rho \right] \quad (1)
\end{aligned}$$

ρ is the initial environment distribution for the start and hideout locations ($s_0 \sim \rho$ is omitted from the derivation), π^d is the diffusion global planner, and \mathbf{w} is the generated waypoints to be tracked, t_g is the number of waypoints. Equation (1) shows that we can decompose our adversarial evading learning problem into a sequential optimization problem, including a waypoint generator and a low-level waypoint tracker, both of which aim to maximize the discounted accumulative reward. However, the unconstrained random exploration of these policies will be subject to high variance from the partial observability; therefore, we confine our exploration in a more reasonable region described by the diffusion policy distribution in the previous section. We set reward terms to guide the evader to follow the waypoint and avoid detection in Equation (2) where r_g is the reward obtained when reaching the waypoint, r_{adv} is the detection penalty, and r_d is the distance penalty to the next waypoint.

$$r = r_g + r_d + r_{adv} \quad (2)$$

C. Cost Map Construction and Inference

Having discussed how the diffusion path planner could help the RL explore within the reward promising region in §IV-B and how the low-level SAC policy could be derived under the global path and initial environment distribution, we now take a step further and describe which global path sample should be drawn in each test case.

TABLE I
DIFFUSION-RL BENCHMARKS (MEAN \pm STD), G: GLOBAL-VIEW MODE, L: LOCAL-VIEW MODE

Domain	Prisoner Escape (G)			Narco Interdiction (G)			Prisoner Escape (L)			Narco Interdiction (L)		
	Score \uparrow	Detection \downarrow	Goal-Reach \uparrow	Score \uparrow	Detection \downarrow	Goal-Reach \uparrow	Score \uparrow	Detection \downarrow	Goal-Reach \uparrow	Score \uparrow	Detection \downarrow	Goal-Reach \uparrow
Non-Learning Approaches												
A-Star Heuristic	0.72 \pm 0.19	0.34 \pm 0.24	0.98 \pm 0.14	0.64 \pm 0.30	0.39 \pm 0.31	0.80 \pm 0.40	0.80 \pm 0.18	0.25 \pm 0.15	1.00 \pm 0.00	0.53 \pm 0.29	0.51 \pm 0.31	0.76 \pm 0.43
RRT-Star Heuristic	0.73 \pm 0.18	0.32 \pm 0.22	0.94 \pm 0.24	0.66 \pm 0.31	0.38 \pm 0.32	0.83 \pm 0.38	0.77 \pm 0.11	0.29 \pm 0.14	1.00 \pm 0.00	0.59 \pm 0.26	0.46 \pm 0.30	0.84 \pm 0.37
VO-Heuristic	0.74 \pm 0.11	0.32 \pm 0.14	0.98 \pm 0.14	0.64 \pm 0.10	0.43 \pm 0.12	1.00 \pm 0.00	0.73 \pm 0.12	0.33 \pm 0.15	0.99 \pm 0.10	0.64 \pm 0.10	0.43 \pm 0.11	1.00 \pm 0.00
Learning Approaches												
DDPG	0.23 \pm 0.34	0.73 \pm 0.40	0.07 \pm 0.26	0.31 \pm 0.32	0.65 \pm 0.37	0.00 \pm 0.00	0.23 \pm 0.34	0.73 \pm 0.40	0.07 \pm 0.26	0.26 \pm 0.36	0.70 \pm 0.42	0.00 \pm 0.00
SAC	0.78 \pm 0.12	0.06 \pm 0.11	0.13 \pm 0.34	0.49 \pm 0.35	0.43 \pm 0.41	0.01 \pm 0.10	0.73 \pm 0.12	0.10 \pm 0.15	0.05 \pm 0.22	0.51 \pm 0.40	0.41 \pm 0.47	0.00 \pm 0.00
Diffusion Only	0.78 \pm 0.09	0.28 \pm 0.12	1.00 \pm 0.00	0.78 \pm 0.13	0.26 \pm 0.15	1.00 \pm 0.00	0.79 \pm 0.10	0.26 \pm 0.13	1.00 \pm 0.00	0.78 \pm 0.13	0.26 \pm 0.15	1.00 \pm 0.00
Our Approaches												
Diffusion-RL	0.90 \pm 0.09	0.12 \pm 0.10	0.96 \pm 0.20	0.89 \pm 0.11	0.12 \pm 0.10	0.94 \pm 0.24	0.90 \pm 0.12	0.11 \pm 0.10	0.90 \pm 0.30	0.89 \pm 0.11	0.11 \pm 0.11	0.91 \pm 0.29
Diffusion-RL-Map	0.94\pm0.08	0.07 \pm 0.08	0.98 \pm 0.14	0.94\pm0.07	0.07 \pm 0.08	1.00 \pm 0.00	0.95\pm0.09	0.05 \pm 0.07	0.95 \pm 0.22	0.94\pm0.08	0.06 \pm 0.07	0.95 \pm 0.22

Even though the evasive agent does not have direct access to the camera or the terrain map information, this agent can still perform reverse spatial inference on the map by interacting with the learned policies to identify regions of heightened risk. Following this idea, we construct a cost map to reflect the risk of detection which we can then use to score the global paths.

Algorithm 4 describes our procedure. We run a certain number of episodes after the hierarchy is trained well (Line 1) and simultaneously record the evader location \mathbf{x} and its distance to the closest searching agent \mathbf{d} (Line 2). If the searching agent is within the evader’s field of view, we select out the evader locations x_i with which the associated distance, d_i , is below a risk threshold ϵ and add a Gaussian distribution whose mean is x_i and standard deviation σ (Line 3-5). Next, we perform normalization and output the map.

Importantly, end-users can preview the global paths before execution or revise the cost map with the newly added global information, which adds more flexibility and interpretability compared with traditional fully MDP-based RL algorithms (Line 6). We can select the global path with the lowest cost based on the costmap (Line 7-8).

Algorithm 4: Costmap and Inference

Data: Initial state s_0 , Diffusion Global Planner π^d ,
Learned local policy π^l , Costmap \mathbf{G} , Evasive agent location \mathbf{x}

Result: Selected global plan \mathbf{w}^*

```

1 while costmap constructing episodes do
     $\triangleleft$  Continue running episodes with learned policies
2  $\mathbf{x}, \mathbf{d} = \text{Env}(s_0, \pi^d, \pi^l)$ 
3 for all  $x_i, d_i$  from  $\mathbf{x}, \mathbf{d}$  do
     $\triangleleft$  Update costmap when search team is close
4     if  $d_i < \epsilon$  & see searching agent then
5          $\mathbf{G} \leftarrow \mathbf{G} + \mathcal{N}(x_i, \sigma^2)$ ;  $\triangleleft$  Add a Gaussian
     $\triangleleft$  Normalize and adjust costmap
6  $\mathbf{G} \leftarrow \text{adjust}(\mathbf{G}/\mathbf{G}_{\max})$ ;
     $\triangleleft$  Get global path samples
7  $\mathcal{T} \leftarrow \{\mathbf{w}_i : \mathbf{w}_i \sim \pi^d(\mathbf{w}|s_0)\}_{i=0}^{N_s}$ ;
     $\triangleleft$  Find global path with lowest cost
8  $\mathbf{w}^* = \arg \max_{\mathbf{w}_i \in \mathcal{T}} \int_{\mathbf{w}_i} \mathbf{G}(w)dw$ ;
```

V. RESULTS & DISCUSSION

In this section, we will first benchmark our diffusion-RL framework for the global- and local-view evader against

both heuristics and learning based baselines (see §V-A). Then we visualize our constructed costmap and show the interpretability, efficiency, and generalizability of our method in multiple ablation studies (see §V-B-§V-D). Next, we validate our hierarchy in the real robot testbed (see §V-E). Finally, we include a result discussion section (see §V-F).

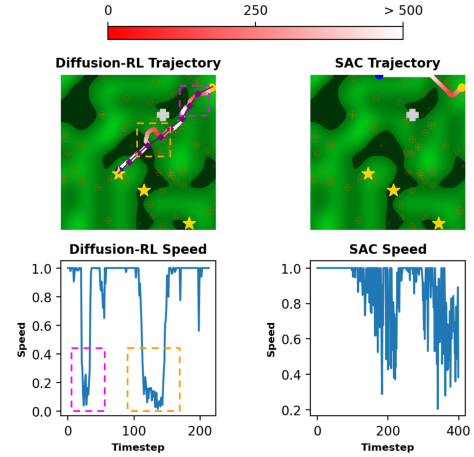


Fig. 3. Our Diffusion-RL trajectory vs SAC trajectory. Colorbar indicates the distance between the evader and closest pursuer and the purple line indicates the diffusion global path.

A. Achieving Long-Term Planning and Short-Term Evasion

We propose to use the following metrics to quantitatively evaluate our method and compare it against the baselines: detection, goal-reaching rate, and score (\uparrow means higher is better and \downarrow means lower is better in Table I). Detection is the average number of steps when the evader is detected for each episode. Goal-reaching rate is the number of episodes in which the evader reaches the goal within the time limit divided by the total number of episodes tested. The score metric is a weighted reward term that balances the two main objectives in our domains: reaching the goal (± 50) and staying undetected by the opposing blue agents (-1 for each detection). Each metric is normalized by the min-max value of each category and we test the algorithms in 100 episodes with different random seeds from the training.

We compare our diffusion+RL method with learning based and non-learning-based baselines. A* and RRT* heuristics are from the open-sourced environment [12] where the evader follows the A* or RRT* path and shows some pre-scripted adversarial behaviors (e.g. heading to dense forest, changing velocity, etc.) when the search team is nearby. Velocity obstacle (VO) method is widely used in dynamic obstacle avoidance tasks which samples a velocity from the

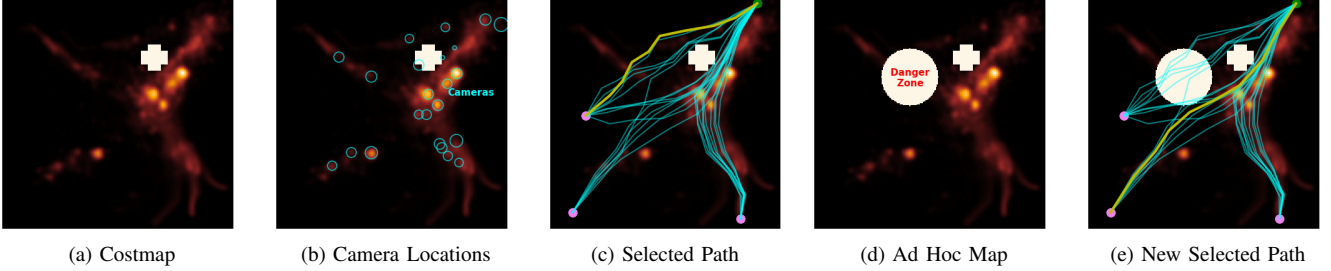


Fig. 4. Path Planning with the Costmap: The costmap (a) is constructed by correlating the agent’s risk of detection to its location on the map. We show in (b) that the agent can successfully identify where the cameras are. Given this costmap, the agent can select a path that best evades high-cost regions (c). Additional obstacles can be added ad-hoc (d) and a new path can be chosen (e). The grey areas indicate untraversable obstacles or danger zones.

collision-free velocity space [47]. From Table I, we find these heuristics can reach the goal at a high rate in two view modes across both domains. However, the heuristic evader is detected by the search team much more than our methods, which leads to a lower score. The main reason is that the evader will be exposed to the cameras hidden from it, which may attract the dynamic search team and the hand-crafted evasive heuristic is not optimal for escaping.

Although RL-only approaches (DDPG [48] & SAC [49]) directly optimize the score as the reward function, our methods outperform them on average by 108% on the score metric across both domains. The SAC evader can be detected less than our diffusion-RL algorithm by 10.26% in prisoner escape domain, which is interesting and a red herring. Figure 3 shows a red colorbar for the distance between the evader and the closest agent in the pursuit team, and the diamond purple line indicates the diffusion planned global path. From the trajectory, we can see the SAC algorithm will lead the evader to the edge of the map where there is no camera but not the goal hideout. Instead, our method can loosely follow the diffusion waypoints (purple diamond) and simultaneously deviate a little to avoid the search team when they are close (indicated by magnet and orange dashed box). In addition, our method learns to reduce the evader speed when evading, which lowers the probability of detection, but maintains a higher speed when safer. We also ablate our diffusion-RL with the diffusion-only baseline (Diffuser [36]) and the 56.6% detection rate decreasing shows the low-level RL policy is crucial to adversarial evading behaviors.

B. Interpretability and Flexibility

As discussed in §IV-C, we build a costmap based on the distance between evader and pursuer which implies detection risks. The costmap serves as an interpretable and memory-efficient way to allow our hierarchical agent to plan based on past experiences and will improve the flexibility in the inference stage compared with RL-only motion planning.

Figure 4a shows the costmap, where the high-intensity region indicates the evader is close to the search team which may lead to detection. We also find that the potential detection usually happens around the cameras (see Figure 4b), which is reasonable since the searching team will search the region after the evader is detected by the camera. Therefore, Figure 4c shows the evasive agent can select the best global

path which receives lowest cost and can best conceal it from the camera array. At the inference stage, we can adjust the costmap with the new information we received. For example, we can add an undesired danger zone for the evader on the costmap (see Figure 4d) such that it will select another way to reach another hideout which will avoid the danger zone (see Figure 4e). We ablate our model with and without the costmap and show that the detection from map-based path selection is further decreased by half.

C. Efficiency and Diversity in Guidance

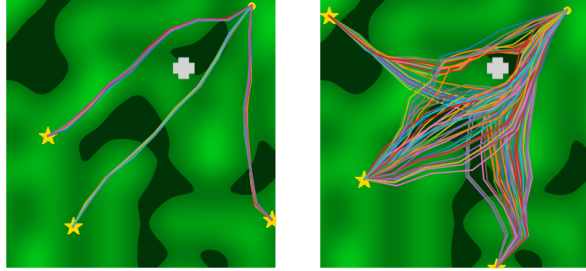
Figure 5a-5b compares the diffusion global paths trained on the datasets from RRT* and A*. We see the diffusion model encodes a more diverse distribution of the paths leading to the final hideouts. As a result, A* guided RL method can only receive a score of 0.78 ± 0.09 , which is worse than the performance of our diffusion-RL method (0.90 ± 0.09). Table 5c shows the planning time in the inference stage for both the diffusion and RRT* algorithms. The diffusion model takes 85.7% less time to generate one trajectory compared with RRT*, which requires a map search. Furthermore, the difference is enlarged when planning more paths since we can draw samples from the diffusion model in parallel. In addition, Figure 5d shows that the diffusion-guided RL training uses less than a half time to reach the same reward level (save 25.2 hours), which greatly improves training time efficiency crucial to parameter tuning. We generate the results using a machine with 11th Gen Intel Core i9 processor and GeForce GTX 1660 Ti graphic card.

D. Generalizability to New Camera Map

The high-level diffusion and low-level RL policies trained on one map can be generalized to other maps with different camera distributions with the only need to re-run costmap reconstruction process rather than the whole training pipeline (see Figure 6). We benchmark with the new camera map, and our results are shown in the Table II. Our method still outperforms the best baseline by 18.6% and outperforms 43.99% across all baselines in average, which shows our algorithm can be generalized to the new camera map without any retraining of diffusion or RL policies.

E. Real Robot Demonstration

We also test our method with the Robotarium [50] testbed to validate our method with real robot dynamics. Figure 7

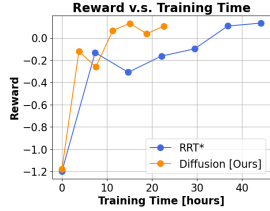


(a) A* Trajectories

(b) Diffusion Trajectories

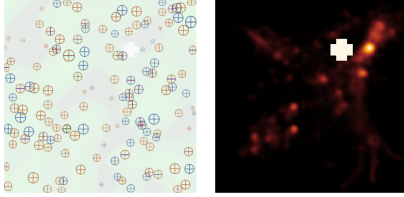
Traj.	RRT*	Diffusion
1	0.7 ± 0.2	0.1 ± 0.0
10	6.2 ± 0.3	0.2 ± 0.0
20	12.5 ± 0.6	0.4 ± 0.1
30	19.7 ± 1.5	0.4 ± 0.0
40	26.3 ± 1.9	0.5 ± 0.0
50	33.0 ± 2.3	0.6 ± 0.2

(c) Inference Time (mean \pm std)



(d) Training Time (Hours)

Fig. 5. The paths from the diffusion model trained on RRT* are more diverse than A* paths (5a-5b). Compared to the traditional RRT* planner, the diffusion model leverages the power of parallel computing to generate trajectories an order of magnitude faster (5c). The diffusion-guided RL training also significantly decreases the training time (5d).



(a) New Camera Map

(b) New Costmap

Fig. 6. (6a) - Cameras are highlighted. We use a different camera distribution in the test scenario (indicated by orange) from the one in the training scenario (indicated by blue). (6b) - we derive a new costmap reflecting the testing scenario camera distribution by running Algorithm 4.

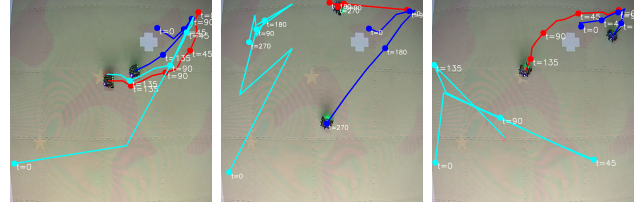
shows the comparison among the RRT* heuristic, SAC, and our method. We find the evader (red trajectory) equipped with our policy can reach the hideout and remain untracked by the searching team (blue and cyan trajectories). In comparison, the SAC policy does not lead the evader to the hideout, and the RRT* heuristic travels a path near cameras and is tracked by the helicopter starting at $t \approx 90$. This validates our benchmarking results and indicates that our hierarchical data-driven learning-based method can outperform the baselines from the efficient diffusion-guided exploration, RL-based trial-and-error multi-agent interaction, and map optimizations.

F. Discussion

The significant disparity in goal-reaching rates between standalone RL and our approaches indicates that RL struggles with long-horizon exploration in large partially observable domains, supporting our premise in §I that diffusion models can guide RL exploration. Additionally, Figure 3 reveals that SAC can become trapped in a local minimum. From this, we infer that our methods can achieve long-term planning by providing the RL agent with a diffusion-based

TABLE II
GENERALIZABILITY BENCHMARKS (MEAN \pm STD)

Domain (global-view)	Prisoner Escape		
	Score \uparrow	Detection \downarrow	Goal-Reach. \uparrow
Non-Learning Approaches			
A-Star Heuristic	0.694 ± 0.185	0.376 ± 0.229	0.970 ± 0.171
RRT-Star Heuristic	0.701 ± 0.179	0.367 ± 0.220	0.970 ± 0.171
VO-Heuristic	0.728 ± 0.104	0.336 ± 0.131	0.980 ± 0.140
Learning Approaches			
DDPG	0.136 ± 0.241	0.847 ± 0.264	0.070 ± 0.255
SAC	0.670 ± 0.203	0.195 ± 0.226	0.130 ± 0.336
Diffusion Only	0.767 ± 0.080	0.292 ± 0.100	1.000 ± 0.000
Our Approaches			
Diffusion-RL [ours]	0.864 ± 0.111	0.155 ± 0.116	0.940 ± 0.237
Diffusion-RL-Map [ours]	0.910 ± 0.075	0.113 ± 0.093	1.000 ± 0.000



(a) RRT* Heuristic

(b) SAC

(c) Diffusion-RL-Map

Fig. 7. Pursuit-evasion trajectories: the evader, search party, and helicopter trajectory are indicated with red, blue, and cyan, respectively. We use a diffusion model to guide the evader to the hideout and explore escaping behaviors with RL, which performs better than RRT* heuristic with insufficient evasive behaviors and SAC method converging to a suboptimal place.

global plan while retaining the agility to evade opponent agents in the short horizon. The ablation studies in §V-B to §V-D demonstrate that our hierarchy can generate more interpretable paths, have more flexible motion plans and generalize to different test maps. Importantly, it significantly improves training and inference efficiency, which unlocks the potential on more applications in real-time tasks [51], [52].

VI. CONCLUSION AND FUTURE WORK

In conclusion, we have presented a novel learning-based framework for evaders in large, partially observable, multi-agent pursuit-evasion settings. Our approach can help the evader reach the hideout and best conceal itself from capturing by using a hierarchy with a high-level diffusion path planner and a low-level RL evasive policy. In the future, we plan to train the whole framework end-to-end and bring our diffusion-RL technique to real-world navigation tasks involving high-level human domain knowledge transfer and low-level dynamic constraints (e.g. environment-aware path generation and finetuning in autonomous driving).

REFERENCES

- [1] R. Vidal, O. Shakernia, H. J. Kim, D. H. Shim, and S. Sastry, "Probabilistic pursuit-evasion games: theory, implementation, and experimental evaluation," *IEEE transactions on robotics and automation*, vol. 18, no. 5, pp. 662–669, 2002.
- [2] W. Silkman, "The use of us naval surface combatants in the maritime counter narcotics interdiction effort: A major impact on the flow of drugs," *Newport, Rhode Island, United States. Retrieved from Naval War College*, 2001.
- [3] Y. A. Hasan, A. Garg, S. Sugaya, and L. Tapia, "Defensive escort teams for navigation in crowds via multi-agent deep reinforcement learning," *IEEE Robotics and Automation Letters*, vol. 5, no. 4, pp. 5645–5652, 2020.
- [4] E. Antonioni, V. Suriani, F. Riccio, and D. Nardi, "Game strategies for physical robot soccer players: A survey," *IEEE Transactions on Games*, vol. 13, no. 4, pp. 342–357, 2021.

- [5] A. Afzalov, A. Lotfi, B. Inden, and M. E. Aydin, "A strategy-based algorithm for moving targets in an environment with multiple agents," *SN Computer Science*, vol. 3, no. 6, p. 435, 2022.
- [6] V. Bulitko and N. Sturtevant, "State abstraction for real-time moving target pursuit: A pilot study," in *AAAI Workshop: Learning For Search*. Citeseer, 2006, pp. 72–79.
- [7] A. I. A. Isaza, J. Lu, V. Bulitko, and R. Greiner, "A cover-based approach to multi-agent moving target pursuit," in *Proceedings of the AAAI Conference on Artificial Intelligence and Interactive Digital Entertainment*, vol. 4, no. 1, 2008, pp. 54–59.
- [8] D. Sigurdson, V. Bulitko, W. Yeoh, C. Hernández, and S. Koenig, "Multi-agent pathfinding with real-time heuristic search," in *2018 IEEE Conference on Computational Intelligence and Games (CIG)*. IEEE, 2018, pp. 1–8.
- [9] J. Kennedy and R. Eberhart, "Particle swarm optimization," in *Proceedings of ICNN'95-international conference on neural networks*, vol. 4. IEEE, 1995, pp. 1942–1948.
- [10] Q. Liu, W. Wei, H. Yuan, Z.-H. Zhan, and Y. Li, "Topology selection for particle swarm optimization," *Information Sciences*, vol. 363, pp. 154–173, 2016.
- [11] Y. Bar-Shalom and X.-R. Li, *Multitarget-multisensor tracking: principles and techniques*. YBs Storrs, CT, 1995, vol. 19.
- [12] S. Ye, M. Natarajan, Z. Wu, R. Paleja, L. Chen, and M. C. Gombolay, "Learning models of adversarial agent behavior under partial observability," 2023.
- [13] S. Ye, M. Natarajan, Z. Wu, and M. Gombolay, "Diffusion based multi-agent adversarial tracking," *arXiv preprint arXiv:2307.06244*, 2023.
- [14] Z. Wu, S. Ye, M. Natarajan, L. Chen, R. Paleja, and M. C. Gombolay, "Adversarial search and tracking with multiagent reinforcement learning in sparsely observable environment," 2023.
- [15] J. Li, C. Tang, M. Tomizuka, and W. Zhan, "Hierarchical planning through goal-conditioned offline reinforcement learning," *IEEE Robotics and Automation Letters*, vol. 7, no. 4, pp. 10216–10223, 2022.
- [16] J. Liu, M. Stamatopoulou, and D. Kanoulas, "Dipper: Diffusion-based 2d path planner applied on legged robots," *arXiv preprint arXiv:2310.07842*, 2023.
- [17] J. Carvalho, A. T. Le, M. Baierl, D. Koert, and J. Peters, "Motion planning diffusion: Learning and planning of robot motions with diffusion models," in *2023 IEEE/RSJ International Conference on Intelligent Robots and Systems (IROS)*. IEEE, 2023, pp. 1916–1923.
- [18] G. Wang, F. Wei, Y. Jiang, M. Zhao, K. Wang, and H. Qi, "A multi-uv maritime target search method for moving and invisible objects based on multi-agent deep reinforcement learning," *Sensors*, vol. 22, no. 21, p. 8562, 2022.
- [19] M. Andrychowicz, F. Wolski, A. Ray, J. Schneider, R. Fong, P. Welinder, B. McGrew, J. Tobin, O. Pieter Abbeel, and W. Zaremba, "Hindsight experience replay," *Advances in neural information processing systems*, vol. 30, 2017.
- [20] P.-L. Bacon, J. Harb, and D. Precup, "The option-critic architecture," in *Proceedings of the AAAI conference on artificial intelligence*, vol. 31, no. 1, 2017.
- [21] P. Zhang, X. Chen, L. Zhao, W. Xiong, T. Qin, and T.-Y. Liu, "Distributional reinforcement learning for multi-dimensional reward functions," 2021.
- [22] S. Nasiriany, H. Liu, and Y. Zhu, "Augmenting reinforcement learning with behavior primitives for diverse manipulation tasks," in *2022 International Conference on Robotics and Automation (ICRA)*. IEEE, 2022, pp. 7477–7484.
- [23] M. Salimi, "A pursuit-evasion game with hybrid system of dynamics," *Mathematical Methods in the Applied Sciences*, 2020.
- [24] Y. Feng, L. Dai, J. Gao, and G. Cheng, "Uncertain pursuit-evasion game," *soft computing*, vol. 24, pp. 2425–2429, 2020.
- [25] R. Vidal, O. Shakhmurov, H. Kim, D. Shim, and S. Sastry, "Probabilistic pursuit-evasion games: theory, implementation, and experimental evaluation," *IEEE Transactions on Robotics and Automation*, vol. 18, no. 5, pp. 662–669, 2002.
- [26] Y. Wang, L. Dong, and C. Sun, "Cooperative control for multi-player pursuit-evasion games with reinforcement learning," *Neurocomputing*, vol. 412, pp. 101–114, 2020.
- [27] J. Selvakumar and E. Bakolas, "Min–max q-learning for multi-player pursuit-evasion games," *Neurocomputing*, vol. 475, pp. 1–14, 2022.
- [28] X. Qu, W. Gan, D. Song, and L. Zhou, "Pursuit-evasion game strategy of usv based on deep reinforcement learning in complex multi-obstacle environment," *Ocean Engineering*, vol. 273, p. 114016, 2023.
- [29] Z. Zhou and H. Xu, "Decentralized optimal large scale multi-player pursuit-evasion strategies: A mean field game approach with reinforcement learning," *Neurocomputing*, vol. 484, pp. 46–58, 2022.
- [30] C. De Souza, R. Newbury, A. Cosgun, P. Castillo, B. Vidolov, and D. Kulić, "Decentralized multi-agent pursuit using deep reinforcement learning," *IEEE Robotics and Automation Letters*, vol. 6, no. 3, pp. 4552–4559, 2021.
- [31] H. Yang, P. Ge, J. Cao, Y. Yang, and Y. Liu, "Large scale pursuit-evasion under collision avoidance using deep reinforcement learning," in *2023 IEEE/RSJ International Conference on Intelligent Robots and Systems (IROS)*. IEEE, 2023, pp. 2232–2239.
- [32] B. Baker, I. Kanitscheider, T. Markov, Y. Wu, G. Powell, B. McGrew, and I. Mordatch, "Emergent tool use from multi-agent autocurricula," *arXiv preprint arXiv:1909.07528*, 2019.
- [33] P. Dhariwal and A. Nichol, "Diffusion models beat gans on image synthesis," *Advances in Neural Information Processing Systems*, vol. 34, pp. 8780–8794, 2021.
- [34] J. Ho, C. Saharia, W. Chan, D. J. Fleet, M. Norouzi, and T. Salimans, "Cascaded diffusion models for high fidelity image generation," *J. Mach. Learn. Res.*, vol. 23, no. 47, pp. 1–33, 2022.
- [35] F.-A. Croitoru, V. Hondru, R. T. Ionescu, and M. Shah, "Diffusion models in vision: A survey," *IEEE Transactions on Pattern Analysis and Machine Intelligence*, 2023.
- [36] M. Janner, Y. Du, J. Tenenbaum, and S. Levine, "Planning with diffusion for flexible behavior synthesis," in *International Conference on Machine Learning*, 2022.
- [37] C. Chi, S. Feng, Y. Du, Z. Xu, E. Cousineau, B. Burchfiel, and S. Song, "Diffusion policy: Visuomotor policy learning via action diffusion," in *Proceedings of Robotics: Science and Systems (RSS)*, 2023.
- [38] L. Gao, J. Ding, W. Liu, H. Piao, Y. Wang, X. Yang, and B. Yin, "A vision-based irregular obstacle avoidance framework via deep reinforcement learning," in *2021 IEEE/RSJ International Conference on Intelligent Robots and Systems (IROS)*. IEEE, 2021, pp. 9262–9269.
- [39] B. Rubí, B. Morcego, and R. Pérez, "Quadrotor path following and reactive obstacle avoidance with deep reinforcement learning," *Journal of Intelligent & Robotic Systems*, vol. 103, pp. 1–17, 2021.
- [40] R. Cimurs, J. H. Lee, and I. H. Suh, "Goal-oriented obstacle avoidance with deep reinforcement learning in continuous action space," *Electronics*, vol. 9, no. 3, p. 411, 2020.
- [41] L. Kästner, T. Buiyan, L. Jiao, T. A. Le, X. Zhao, Z. Shen, and J. Lambrecht, "Arena-rosnav: Towards deployment of deep-reinforcement-learning-based obstacle avoidance into conventional autonomous navigation systems," in *2021 IEEE/RSJ International Conference on Intelligent Robots and Systems (IROS)*. IEEE, 2021, pp. 6456–6463.
- [42] P. Hungerländer, "Discrete-time dynamic noncooperative game theory," 2014.
- [43] M. Sani, B. Robu, and A. Hably, "Pursuit-evasion game for nonholonomic mobile robots with obstacle avoidance using nmpe," in *2020 28th Mediterranean conference on control and automation (MED)*. IEEE, 2020, pp. 978–983.
- [44] K. E. C. Booth, C. Piacentini, S. Bernardini, and J. C. Beck, "Target search on road networks with range-constrained uavs and ground-based mobile recharging vehicles," *IEEE Robotics and Automation Letters*, vol. 5, no. 4, pp. 6702–6709, 2020.
- [45] A. I. A. Isaza, J. Lu, V. Bulitko, and R. Greiner, "A cover-based approach to multi-agent moving target pursuit," in *Proceedings of the AAAI Conference on Artificial Intelligence and Interactive Digital Entertainment*, vol. 4, no. 1, 2008, pp. 54–59.
- [46] Z. Wu, S. Ye, M. Natarajan, L. Chen, R. Paleja, and M. C. Gombolay, "Adversarial search and tracking with multiagent reinforcement learning in sparsely observable environment," in *2023 International Symposium on Multi-Robot and Multi-Agent Systems (MRS)*, 2023, pp. 43–49.
- [47] P. Fiorini and Z. Shiller, "Motion planning in dynamic environments using velocity obstacles," *The international journal of robotics research*, vol. 17, no. 7, pp. 760–772, 1998.
- [48] T. P. Lillicrap, J. J. Hunt, A. Pritzel, N. Heess, T. Erez, Y. Tassa, D. Silver, and D. Wierstra, "Continuous control with deep reinforcement learning," *arXiv preprint arXiv:1509.02971*, 2015.
- [49] T. Haarnoja, A. Zhou, P. Abbeel, and S. Levine, "Soft actor-critic: Off-policy maximum entropy deep reinforcement learning with a stochastic actor," in *International conference on machine learning*. PMLR, 2018, pp. 1861–1870.

- [50] S. Wilson, P. Glotfelter, L. Wang, S. Mayya, G. Notomista, M. Mote, and M. Egerstedt, "The robotarium: Globally impactful opportunities, challenges, and lessons learned in remote-access, distributed control of multirobot systems," *IEEE Control Systems Magazine*, vol. 40, no. 1, pp. 26–44, 2020.
- [51] Z. Wu, Z. Zaidi, A. Patil, Q. Xiao, and M. Gombolay, "Learning wheelchair tennis navigation from broadcast videos with domain knowledge transfer and diffusion motion planning," 2024. [Online]. Available: <https://arxiv.org/abs/2409.19771>
- [52] K. M. Lee, S. Ye, Q. Xiao, Z. Wu, Z. Zaidi, D. B. D'Ambrosio, P. R. Sanketi, and M. Gombolay, "Learning diverse robot striking motions with diffusion models and kinematically constrained gradient guidance," *arXiv preprint arXiv:2409.15528*, 2024.